Kidney International, Vol. 48 (1995), pp. 1420–1426

Effect of acid/base balance on H-ATPase 31 kD subunit mRNA levels in collecting duct cells

GÉZA FEJES-TÓTH and ANIKÓ NÁRAY-FEJES-TÓTH

Department of Physiology, Dartmouth Medical School, Lebanon, New Hampshire, USA

Effect of acid/base balance on H-ATPase 31 kD subunit mRNA levels in collecting duct cells. The cortical collecting duct (CCD) adapts to disturbances of acid/base balance by adjusting the direction and magnitude of its HCO_3 transport. The molecular events involved in this adaptation are incompletely understood, but it seems that adaptation is accompanied by changes in the activity and intracellular distribution of the vacuolar H-ATPase. The goal of this study was to examine the effects of metabolic acidosis and alkali load on the expression of the mRNA encoding the 31 kD subunit of the vacuolar H-ATPase in rabbit CCD cells. Pairs of rabbits received either a NH_4Cl load or a $NaHCO_3$ load for 16 hours, resulting in a urinary pH of 5.53 ± 0.38 and 8.42 ± 0.10, respectively. CCD cells were isolated by immunodissection and mRNA levels of the H-ATPase 31 kD subunit and of β-actin were determined from the same cDNA samples by quantitative RT-PCR. H-ATPase mRNA levels were significantly higher in CCD cells from acidotic than alkali-loaded rabbits (2.51 ± 1.3 vs. 0.65 ± 0.2; $P < 0.05$). Similar differences in the H-ATPase 31 kD subunit mRNA levels were observed by Northern blotting. β-actin mRNA levels were comparable in CCD cells of the two groups. The distribution of the H-ATPase 31 kD subunit mRNA was determined among the three cell types of the CCD, that is in α- and β-intercalated cells (α-ICC and β-ICC) and principal cells (PC) isolated by fluorescence-activated cell sorting. The level of expression was comparable in α-ICCs and β-ICCs, whereas PCs contained very low levels of H-ATPase mRNA. In both α-ICC and β-ICC the levels of the 31 kD H-ATPase mRNA were significantly higher in acidotic than in alkali-loaded rabbits. These results indicate that in the rabbit CCD changes in acid/base balance not only regulate the subcellular distribution of the vacuolar H-ATPase but also alter its expression, at least at the mRNA level.

Renal adaptation to changes in acid/base balance involves both proximal and distal nephron segments. The cortical collecting duct (CCD) plays a major role in the distal adaptation. The CCD, depending on the acid-base status of the organism, can either secrete or reabsorb HCO_3 as first demonstrated by McKinney and Burg [1, 2]. These opposite transport processes take place in two subtypes of intercalated cells (ICCs): HCO_3 reabsorption occurs in α-ICCs, which are endowed with an apical H-ATPase and a basolateral Cl/HCO_3 exchanger, while HCO_3 secretion occurs in the β-ICC, which is modelled with a basolateral H-ATPase and an apical Cl/HCO_3 exchanger (cf. [3]).

Although the molecular events of the adaptive responses are still incompletely understood, several lines of evidence suggest that at least two key transporters of distal H^+- and HCO_3-transport are involved in this response. Recent observations indicate that the levels of mRNA encoding the basolateral anion exchanger-1 of α-ICCs (AE1 or band 3) are increased in CCD cells in respiratory [4] and metabolic [5] acidosis, and similar changes were observed at the protein level in CCD cells of rabbits with metabolic acidosis [5]. In addition, the subcellular distribution of AE1 is also affected in metabolic acidosis: there is an increase in the amount of AE1 in the basolateral membrane of α-ICCs at the expense of an intracellular vesicular pool [6]. Similarly, immunocytochemical observations indicate that the vacuolar H-ATPase also participates in the adaptation to changes in acid/base balance [6, 7]. Both in the rat and in the rabbit acid loading enhanced the number of intercalated cells exhibiting strong apical staining with an antibody against the 31 kD subunit of the vacuolar H-ATPase, suggesting enhanced insertion of H-ATPase molecules into the apical membrane [6, 7].

In addition to these changes in the intracellular distribution of the vacuolar H-ATPase, several groups demonstrated that NEM-sensitive ATPase activity is increased in the CCD in rats subjected to acidosis and is decreased following alkalosis [8–11]. The mechanisms involved in these changes in H-ATPase activity are not known, and the question whether they are due to changes in *de novo* synthesis of the H-ATPase mRNA is still unanswered. Thus far the only study that investigated H-ATPase mRNA levels following chronic acidosis or alkalosis in the rat kidney found only small changes with either intervention [7]. However, in that study mRNA and protein levels were determined in the whole cortex and medulla; thus, changes in mRNA levels occurring in the CCD might have been obscured. The goal of this study was to examine if steady-state mRNA levels of the vacuolar H-ATPase 31 kD subunit are regulated by metabolic disturbances of acid/base balance in the two intercalated cell types of the CCD. Our results indicate that mRNA levels encoding the H-ATPase 31 kD subunit are significantly increased in CCD cells isolated from rabbits subjected to metabolic acidosis versus metabolic alkalosis, and both α- and β-ICCs participate in this response.

Methods

Animals

Male New Zealand white rabbits, weighing 1.5 to 2.0 kg, were used. The animals were kept on standard diet and had access to water *ad libitum*. Metabolic acidosis was produced by an intragastric load of 15 mmol/kg of NH_4Cl, and alkali loading was achieved by an i.v. infusion of 15 mmol/kg of $NaHCO_3$. Both interventions were done 16 to 20 hours before sacrifice. To keep the amount of Na^+ load constant, rabbits receiving NH_4Cl load also received 15 mmol/kg NaCl, i.v. For the last 12 hours before the experiments the rabbits were on restricted food intake (3 oz). Urine samples were taken from the bladder and blood samples from the ear

artery immediately before sacrifice for the determination of urinary pH and blood gases, respectively.

Cell isolation

CCD cells were isolated from the renal cortex by solid phase immunoadsorption, using a monoclonal antibody against an ectoantigen on these cells, as described previously [12, 13]. The immunodissected CCD cells were further fractionated into the three collecting duct cell types (that is, α- and β-ICCs and principal cells) by fluorescence-activated cell sorting using cell specific markers as described [14, 15]. Principal cells were identified with an FITC-conjugated antibody that reacts specifically with these cells (DT.17; [14]), β-ICCs with peanut lectin agglutinin (PNA) coupled to phycoerythrin, as described in detail elsewhere [14, 15], whereas α-ICCs were operationally defined as the DT 17- and PNA-negative population. To aid in the discrimination between live and dead cells, CCD cell preparations were also stained with DAPI (0.1 μg/ml) which is excluded from viable cells. Using monoclonal antibody (MAb) ST.9 (PC-specific; [12]) and MAb 342 (reacts with connecting tubule cells), we observed only negligible (<1%) contamination of β-ICC preparations with PC and connecting tubule cells, whereas α-ICC preparations contained 2% PC and 16% connecting tubule cells. Immunocytochemistry with MAb IVF12 (anti-band 3; [16]) revealed that the percentage of band 3-positive cells was ~3%, ~1% and 79% in the PC, β-ICC and α-ICC preparations, respectively. Staining of sorted cells with MAb B63 (a β-ICC marker; [17]) revealed that 99% of sorted β-ICC, 2% of sorted α-ICC and <1% of sorted PC were positive for B63.

RNA isolation and cDNA synthesis

Total RNA was isolated using TRI Reagent™ (Molecular Research Center, Inc., Cincinnati, OH). RNA concentrations were calculated from the absorbance measured at 260 nm. cDNA was synthesized using 0.5 to 2 μg of total RNA and 200 U/μg RNA of MMLV reverse transcriptase (Gibco, BRL, Gaithersburg, MD). The reaction mixture also contained 50 mM Tris-HCl (pH 8.3), 75 mM KCl, 10 mM DTT, 3 mM $MgCl_2$, 0.5 mM of each dGTP, dATP, dTTP and dCTP, 20 U RNasin (Promega, Madison, WI) and 3.3 μM random $pd(N)_6$ primers (Boehringer Mannheim, Indianapolis, IN). Following denaturation of the RNA at 75°C for 3 minutes and annealing of primers at room temperature for 10 minutes, reverse transcription was carried out at 42°C for 60 minutes, and then the reaction was terminated by heating the tubes to 75°C for 10 minutes.

Primer selection for the 31 kD subunit of the vacuolar H-ATPase

Sense and antisense degenerate PCR primers were designed based on the published nucleotide sequence of the bovine 31 kD H-ATPase subunit [18]. The oligonucleotide sequences used as primers are as follows. Primer U1: 5′-CA(GA)AT(ACT)AA(GA)CA(CT)ATGA-TGG-3′; primer U2: 5′-AA(GA)GCIGA(GA)GA(GA)TT(CT)AA; primer L1: 5′-ACIA(GA)IGG(GA)AA(GA)TC(CT)TG(CT)TT-3′; primer L2: 5′-AC(CT)TCIGGCATCAT(CT)TG(CT)TG-3′. Primers U1 and L2 were used for determining H-ATPase mRNA levels and bracket a 602 bp PCR product, whereas primers U2 and L1, which bracket a 335 bp PCR product, were used for nested PCR.

PCR amplification

Reactions were performed in a 20 μl total volume containing 10 mM Tris-HCl, pH 8.3, 50 mM KCl, 1.5 mM $MgCl_2$, 75 μM dNTP, 200 nM of each primer, 0.1 U *Taq* polymerase (Perkin Elmer) and 1 μCi [^{32}P]dCTP (NEN, 3000 Ci/mmol) with four 1:4 serial dilutions (0.0625 to 4 ng) of template cDNA. Each sample was overlayed with 20 μl of Chill-Out™ (MJ Research, Inc., Watertown, MA) to prevent evaporation. After an initial 2 minutes denaturation at 96°C, PCR was carried out for 25 cycles with denaturation at 95°C for 1 minute, annealing at 54°C for 1 minute and primer extension at 72°C for 1 minute. The reaction mixtures were incubated for a final extension at 72°C for 8 minutes. The relative abundance of β-actin mRNA in each CCD cell sample was determined using primers and conditions as described [5]. cDNA samples derived from pairs of rabbits (acidotic/alkalotic) were always amplified simultaneously in the same PCR.

After amplification, 4 μl tracking dye was added to each sample, and 20 μl was run on a 6% polyacrylamide gel. Gels were dried and the amount of radioactivity in the PCR products determined using a model 425 PhosphorImager™ (Molecular Dynamics, Sunnyvale, CA). The relative abundance of the H-ATPase 31 kD subunit mRNA was determined by measuring [^{32}]dCTP incorporation into the 602 bp H-ATPase and the 351 bp β-actin PCR products using increasing amounts of cDNA, and calculating the ratio of the resulting slopes.

DNA sequencing

The nested PCR product generated using primers U2 and L1 and rabbit CCD cDNA as template was extracted by phenol/chloroform, and unincorporated primers and nucleotides were removed by centrifugal diafiltration using a Microcon-100 ultrafiltration unit (Amicon Inc., Beverly, MA). Sequencing was performed by the Dye Deoxy Terminator chemistry on an ABI 373A automated sequencer.

A computer-assisted database search was performed at the National Center for Biotechnology Information (NCBI) using the BLAST network service [19].

Northern blot analysis

Northern blotting was carried out using standard protocols [20]. In brief, 1.5 μg poly(A)$^+$RNA originating from immunodissected CCD cells from acidotic and control rabbits was fractionated on a 1.2% agarose gel containing 1.1% formaldehyde. RNA was transferred to a nylon membrane (0.45 μm; MSI Inc., Westborough, MA) and probed with a gel-purified PCR fragment generated with primers U1 and L2 labeled with ^{32}P during the PCR. Prehybridization was performed at 42°C for 10 to 12 hours in 5× SSC, 5× Denhart's solution, 50% formamide, 100 μg/ml salmon sperm DNA and 0.5% SDS. Hybridization was done using the same conditions as for prehybridization for 12 hours. Two washes were carried out at room temperature for 15 minutes each, with 1× SSC, 0.1% SDS, followed by two washes with 0.25× SSC, 0.1% SDS. After a final wash at 45°C for 15 minutes with 0.1× SSC, 0.1% SDS, the blot was exposed to X-ray film. The blot was stripped by incubating it in 0.1% SDS, 2 mM Tris (pH 8.3), 1 mM EDTA at 75°C for 45 minutes, and then re-probed for β-actin using a ^{32}P-labeled cRNA probe transcribed from a 250 bp mouse β-actin template (Ambion, Austin, TX). Prehybridization and

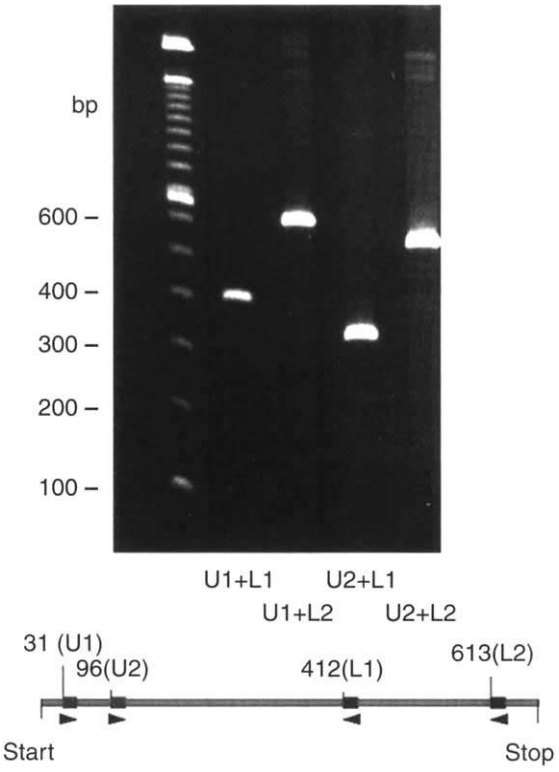

Fig. 1. *Representative RT-PCR of H-ATPase 31 kD subunit.* RT-PCR was performed with 5 ng of rabbit CCD cDNA using the outer primers U1 and L2 (lane 2). Nested PCR was performed using a 1: 5,000-fold dilution of the 602 bp PCR product shown in lane 2 and primers U1 and L1 (lane 1), U2 and L1 (lane 3) and U2 and L2 (lane 4). The expected size of the PCR product using primers U1 and L1 is 381 bp, with primers U2 and L1 is 335 bp and primers U2 and L2 is 517 bp. The positions of the primers on the bovine vacuolar H-ATPase are shown on the bottom part of the figure. The positions of the molecular weight standards are shown on the left.

hybridization for β-actin was done as for H-ATPase, but at 55°C, and washes were done at 60°C.

Results

Quantitative RT-PCR of the 31 kD subunit of H-ATPase from rabbit CCD cells

Using sense and antisense degenerate oligonucleotide primers (designated U1 and L2), an approximately 600 bp PCR product was amplified using cDNA derived from immunodissected rabbit CCD cells (Fig. 1, lane 2). This PCR product is of the predicted size (602 bp) based on the published sequence of the bovine 31 kD subunit of the vacuolar H-ATPase [18]. The identity of this PCR product was verified by two methods: (a) by nested PCR and (b) by direct sequencing of the nested PCR product. Nested PCR was performed by using sense and antisense primers with start positions corresponding to nucleotides 96 and 412, respectively, in the bovine H-ATPase (primers U2 and L1). The nested primer pair yielded the expected size (335 bp) PCR product (Fig 1, lane 3), indicating that the 602 bp product is indeed amplified from H-ATPase cDNA. Other primer pair combinations (U1 and L1 and U2 and L2) also yielded the expected size products (381 and 517 bp; Fig. 1, lanes 1 and 4). When RNA from the same preparation, as used for reverse transcription, was included instead of cDNA as template ("no RT control") no PCR product was detected under the same conditions (data not shown).

To further verify the identity of the 602 bp amplicon, it was subjected to direct sequencing from both directions using primers U2 and L1. Comparison of the obtained nucleotide sequence to the corresponding region of the bovine 31 kD subunit cDNA revealed a 92% identity, and 100% identity at the level of the predicted amino acid sequence (Fig. 2).

Effect of metabolic acidosis and alkali loading on the H-ATPase 31 kD subunit mRNA levels in rabbit CCD cells

To examine whether changes in acid/base balance result in an altered expression of the 31 kD H-ATPase mRNA, we performed acid loads or alkali loads in pairs of rabbits. Urinary pH averaged 5.53 ± 0.38 in acidotic versus 8.42 ± 0.10 in alkali-loaded rabbits ($P < 0.001$). mRNA levels for the H-ATPase 31 kD subunit and for β-actin were determined in cDNAs derived from isolated CCD cells. The levels of the H-ATPase 31 kD subunit mRNA were markedly higher in CCD cells of acidotic versus alkali-loaded animals, whereas the levels of β-actin mRNA did not change significantly in the two groups. Consequently, the relative abundance of the H-ATPase 31 kD subunit mRNA, calculated from the ratio of [^{32}]dCTP incorporated into the 602 bp PCR product and into the 350 bp β-actin PCR product was significantly higher in acidotic than in alkali-loaded animals (Fig. 3). The average increase was ~4.5-fold. This difference was confirmed by Northern blotting of CCD mRNAs obtained from acidotic and alkalotic rabbits using the labeled PCR product as probe (Fig. 4). In both cases a single hybridizing mRNA species was detected with a size of approximately 1.3 kb, and its intensity was significantly higher in the CCD cells of acidotic than alkalotic rabbits, whereas reprobing the blot for β-actin resulted comparable signals in the two lanes (Fig. 4).

Effect of acidosis and alkali loading on H-ATPase mRNA levels in different CCD cell subtypes

The distribution of the H-ATPase 31 kD subunit mRNA among three cell types of the CCD (that is α-ICC, β-ICC, and PC) was examined by determining steady-state mRNA levels in these cells after isolating them by fluorescence-activated cell sorting. As shown on Figure 5A, α-ICC and β-ICC expressed comparable levels of H-ATPase mRNA, whereas this mRNA was barely detectable in PCs. When the levels of the H-ATPase 31 kD subunit mRNA were compared in the different cell types originating from acidotic versus alkali-loaded rabbits, we found that both α-ICC and β-ICC expressed higher levels in acidotic rabbits, although due to the large scatter of the data, the differences between the absolute values of H-ATPase mRNA levels in acidosis versus alkalosis did not reach statistical significance (individual data are shown in Fig. 5B). However, comparison between acidotic versus alkali-loaded animal pairs revealed significant differences (average increase in pairs of acidotic versus alkalotic rabbits was 12.4-fold in α-ICC ($P < 0.01$) and 3.6-fold in β-ICC ($P < 0.05$), suggesting that changes in acid/base balance are not accompanied by opposite changes in the H-ATPase mRNA expression in HCO_3-secreting versus HCO_3-reabsorbing intercalated cells.

```
RB CCD:    1 CATCGAGAAAGGTCGTCTTGTGCAAACCCAGAGATTGAAGATTATGGAATACTATGAGAA 60
             ||| |||||||||||||||| ||||||| ||| |||||||||||||||| ||||||||
BOVINE:  192 CATTGAGAAAGGTCGTCTTGTCCAAACCCAAAGACTGAAGATTATGGAATATTATGAGAA 251

RB CCD:   61 GAAAGAAAAGCAGATTGAGCAGCAGAAGAAAATTCAGATGTCCAATTTGATGAATCAAGC 120
             ||||||||||||||||||||||||||||||||||||||||||||||||||||||||||||
BOVINE:  252 GAAAGAAAAGCAGATTGAGCAGCAGAAGAAAATTCAGATGTCCAATTTGATGAATCAAGC 311

RB CCD:  121 AAGGCTGAAAGTCCTCAGAGCAAGAGATGATCTTATCACAGACCTTCTAAATGAAGCAAA 180
             ||||| |||||||||||||| |||||||| |||||||||||||| |||||||||||||
BOVINE:  312 GAGGCTCAAAGTCCTCAGAGCGAGAGATGACCTTATCACAGACCTACTAAATGAAGCAAA 371

RB CCD:  181 ACAGAGACTCAGCAAGGTGGTGAAAGACACAACCAGGTACCAAGTGCTGCTCGATGGATT 240
             |||||||||||||| |||| |||| |||||||||||||||||||| |||||| |
BOVINE:  372 ACAGAGACTCAGCAAAGTGGTAAAAGATACAACCAGGTACCAAGTGCTGCTGGATGGACT 431

RB CCD:  241 GGTCCTCCAGGGTTTATACCAGTTGTTGGAGCCCAGAATGATTGTTCGTTGCAGG 295
             |||||||||||||| ||||||||| |||||||| | ||||| ||||| ||||||
BOVINE:  432 GGTCCTCCAGGGTTTGTACCAGTTGCTGGAGCCCCGGATGATCGTTCGCTGCAGG 486
```

Fig. 2. *Alignment of the nucleotide sequence of rabbit (RB) CCD H-ATPase 31 kD subunit with the corresponding region of bovine vacuolar H-ATPase.* Vertical lines indicate identity between the rabbit CCD and bovine vacuolar H-ATPase. Identities = 273/295 (92%), positives = 274/295 (92%).

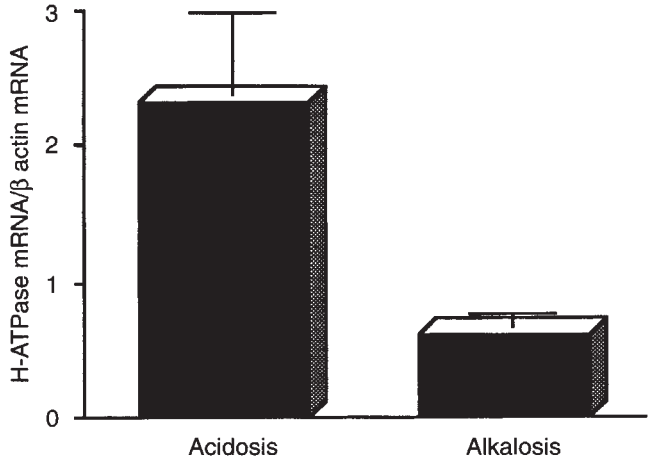

Fig. 3. *Expression of H-ATPase 31 kD subunit mRNA in CCD cells isolated from acidotic and alkalotic rabbits.* RT-PCR was performed with 4 different amounts (0.0625–4 ng) of CCD cDNA isolated from rabbits subjected to metabolic acidosis or alkalosis for 16 to 20 hours as described under **Methods**. Values shown are relative amounts that were corrected for the levels of β-actin. $N = 13$ rabbits in each group. Data are means ± SEM. $^*P < 0.01$ using Wilcoxon test.

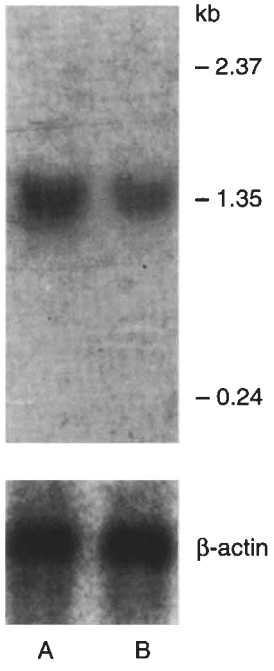

Fig. 4. *Northern blot analysis of the expression of H-ATPase 31 kD subunit mRNA in CCD cells.* 1.5 μg poly(A)$^+$RNA isolated from immunodissected CCD cells from acid-loaded (**A**) and base-loaded (**B**) rabbits was analyzed as described under **Methods**. After an autoradiogram was taken, the blots were stripped and re-probed for β-actin. The positions of molecular weight standards are shown on the left.

Discussion

The vacuolar H-ATPase is a key enzyme in distal acid/base transport. This enzyme can occur with either apical or basolateral polarity in HCO_3-reabsorbing α-ICCs and HCO_3-secreting β-type ICCs, respectively (cf. [3]). The exact molecular and cellular mechanisms responsible for the changes in H^+ transport in the CCD during disturbances of acid/base homeostasis have not yet been elucidated, but intracellular redistribution of the vacuolar H-ATPase in intercalated cells is thought to be the major adaptive response [6, 7, 21]. There is evidence for increased incorporation of H-ATPase molecules into the apical membrane of rat α-ICCs after metabolic acidosis [6, 7]. Changes in the intracellular distribution of H-ATPase in the CCD in metabolic alkalosis are less obvious, as the percentage of cells with well-polarized basolateral H-ATPase staining did not increase significantly during a 14-day alkali load [7].

In addition to these changes in the intracellular distribution of H-ATPase, there is evidence that H-ATPase activity normalized for tubule length also changes with acidosis and alkalosis in the CCD [8–11], suggesting alterations in cellular H-ATPase content. The biochemical mechanism underlying the observed changes in H-ATPase activity is not clear, but it is possible that similarly as with AE1, another key enzyme of distal acid/base transport, metabolic acidosis or alkalosis results in changes in mRNA expression [4, 5]. The results of the present study clearly demonstrate that the levels of the mRNA encoding the 31 kD subunit of the vacuolar H-ATPase are significantly higher in CCD cells originating from rabbits following a relatively short-term (~16 hrs) metabolic acidosis versus alkali load. These results suggest

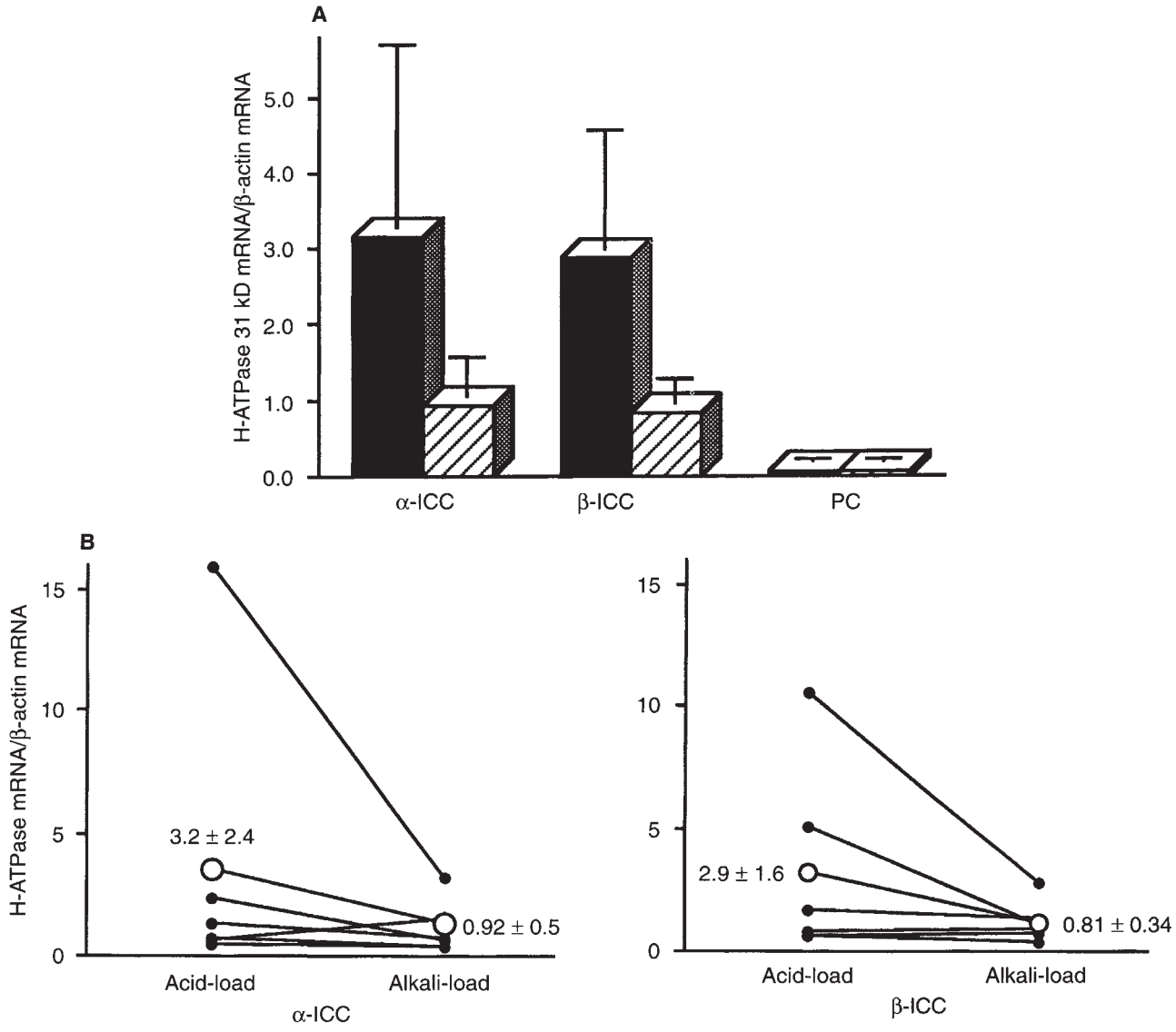

Fig. 5. *Expression of H-ATPase 31 kD subunit mRNA in intercalated cells isolated from acidotic and alkalotic rabbits.* **A.** RT-PCR was performed with 4 different amounts (0.125 to 8 ng) of cDNA derived from α-intercalated (α-ICC), β-intercalated (β-ICC) and principal cells (PC) isolated by fluorescence activated cell sorting from rabbits subjected to metabolic acidosis (■) or alkali-loaded (▨) for 16 to 20 hours. β-actin mRNA levels were determined from each cDNA preparation as described under **Methods**. Values shown are relative amounts that were corrected for β-actin. $N = 6$ for α- and β-ICC, and $N = 4$ for PC. Data are means ± SEM. **B.** Individual values of H-ATPase 31 kD subunit mRNA levels corrected for β-actin (●), and means (○) in sorted α- and β-ICC.

that changes in mRNA synthesis and/or stability in CCD cells in metabolic acidosis or alkalosis might contribute to the changes in H-ATPase activity observed earlier [8–11]. Our observations are at odds with the conclusion reached by an earlier study by Bastani et al who also investigated the relative amount of the H-ATPase 31 kD subunit mRNA after chronic (up to 14 days) acid and alkali load in rat total cortex and medulla using dot blot analyses [7]. Although these authors found slightly increased levels of the H-ATPase 31 kD subunit mRNA in the cortex following acidosis, the increase did not reach statistical significance, and thus they concluded that changes in mRNA levels probably do not play a major role in the adaptive response of the CCD. In the medulla, both metabolic acidosis and alkalosis resulted in a significant, 1.5 to 2-fold increase in H-ATPase mRNA levels 3 and 7 days after acid or alkali load, but no significant changes were observed at the other time points. At the same time, the percentage of cells with well-polarized apical staining for the H-ATPase 31 kD subunit increased from 35% to 48%, while cells with well-polarized basolateral staining decreased from 1.2 to 0.1% in the CCD after 3 days of acid load, and further statistically significant changes were observed at other time points during the 14-day period.

The differences between mRNA levels in CCD cells from acidotic versus alkali-loaded animals are larger in our study than those observed by Bastani et al [7]; however, a direct comparison

between the two studies is difficult for the following reasons. First, our experiments were conducted in rabbits, a species that is adapted to excrete bicarbonate at high rates even under "normal" conditions (urine pH above 8), and thus probably excreted the administered bicarbonate load very quickly, whereas Bastani et al studied rats, which excrete a more acidic urine under control conditions (pH 5 to 6.5). More importantly, we determined mRNA expression in pure populations of CCD cells, whereas in their study mRNA levels were measured in total RNA prepared from unfractionated cortex or medulla. Since vacuolar ATPase is present in several other renal cell types, including proximal tubules which constitute the bulk of the renal cortical tissue, changes in the H-ATPase 31 kD subunit mRNA levels taking place in intercalated cells might have been obscured in that study [7].

Our measurements of mRNA levels encoding the H-ATPase 31 kD subunit in the different cell types comprising the CCD indicate that the levels are comparable in the two ICC subtypes but very low in PCs. These results are in full agreement with immunohistochemical data on the distribution of the H-ATPase 31 kD subunit protein among these cells [7, 22, 23]. If H-ATPase participates both in the apical H^+ extrusion in α-ICCs and in the basolateral H^+ extrusion in β-ICCs, as seems to be the case in the rat [22, 23], then one would expect an opposite regulation by changes in acid/base balance in the two ICC subtypes, that is acidosis would increase H-ATPase in α-ICC, and alkalosis would do the same in β-ICC. Our results, however, indicate that the H-ATPase 31 kD subunit mRNA levels are significantly higher in acidotic than in alkali-loaded rabbits in both α-ICC and β-ICC. This suggests that, at least in the rabbit, the expression of H-ATPase mRNA is not regulated in opposite directions in HCO_3-secreting and HCO_3-reabsorbing ICC subtypes by acidosis or alkalosis, and raises the possibility that the vacuolar H-ATPase might not contribute significantly to basolateral H^+ extrusion in β-ICCs in the rabbit CCD. This suggestion is in full agreement with an earlier report by Schuster et al [24] in which no significant basolateral staining for the vacuolar H-ATPase 31 kD was observed in rabbit β-intercalated cells. In this context it is interesting to note that recent functional data by Gifford et al indicate that even in the rat, where there is unequivocal histochemical evidence for a basolateral H-ATPase [22, 23], stimulated HCO_3 secretion in the CCD might be mediated by a basolateral H-K-ATPase [25], although the use of the membrane permeant inhibitor SCH28080 precludes unequivocal localization of H-K-ATPase to the basolateral membrane. Consequently, the exact role of H-ATPase in β-ICC remains a matter for speculation at this stage. It is possible that H-ATPase in these cells might subserve functions other than transcellular H^+ transport, like regulation of intracellular pH or intravesicular acidification. Alternatively, the intracellular vesicular pool of this enzyme may represent a "reservoir" that can be recruited into the apical membrane during acidosis. Such apical targeting of H pumps in β-ICC might be responsible for the increase in the number of acid-secreting cells during acidosis [21]. Our observation that the levels of the H-ATPase 31 kD subunit mRNA in β-ICC seem to be increased rather than decreased is compatible with this hypothesis.

In summary, our results demonstrate that mRNA levels encoding the 31 kD subunit of the vacuolar H-ATPase are significantly higher in isolated CCD cells originating from rabbits with metabolic acidosis than from alkali-loaded animals, and similar changes occur in both ICC subtypes. These data suggest that in addition to a cellular redistribution of existing H-ATPase molecules, *de novo* synthesis of H-ATPase might also contribute to the adaptive responses occurring in collecting duct ICCs during metabolic acidosis and alkalosis.

Acknowledgment

This work was supported by NIH Grants DK 39523, DK 45647 and DK 41841. Part of this work was presented at the 27th Annual Meeting of The American Society of Nephrology, October 1994, in Orlando, Florida.

Reprint requests to Dr. Géza Fejes-Tóth, Department of Physiology, Dartmouth Medical School, Borwell Building, 1 Medical Center Drive, Lebanon, New Hampshire 03756-0001, USA.

References

1. McKinney TD, Burg MB: Bicarbonate absorption by rabbit cortical collecting tubules *in vitro*. *Am J Physiol* 234:F141–F145, 1978
2. McKinney TD, Burg MB: Bicarbonate secretion by rabbit cortical collecting tubules *in vitro*. *J Clin Invest* 61:1421–1427, 1978
3. Schuster VL: Function and regulation of collecting duct intercalated cells. *Annu Rev Physiol* 55:267–288, 1993
4. Da Silva JCT Jr, Perrone RD, Johns CA, Madias NE: Rat kidney band 3 mRNA modulation in chronic respiratory acidosis. *Am J Physiol* 260:F204–F209, 1991
5. Fejes-Tóth G, Rusvai E, Moser T, Chen WR, Náray-Fejes-Tóth A: Differential expression of AE1 (band 3) mRNA in renal HCO_3 secreting and reabsorbing intercalated cells. *J Biol Chem* 269:26717–26721, 1994
6. Verlander JW, Madsen KM, Cannon JK, Tisher CC: Activation of acid-secreting intercalated cells in rabbit collecting duct with ammonium chloride loading. *Am J Physiol* 266:F633–F645, 1994
7. Bastani B, Purcell H, Hemken P, Trigg D, Gluck S: Expression and distribution of renal vacuolar proton-translocating adenosine triphosphatase in response to chronic acid and alkali loads in the rat. *J Clin Invest* 88:126–136, 1991
8. Garg LC, Narang N: Stimulation of an N-ethylmaleimide-sensitive ATPase in the collecting duct segments of the rat nephron by metabolic acidosis. *Can J Physiol Pharmacol* 63:1291–1296, 1985
9. Garg LC, Narang N: Decrease in N-ethylmaleimide-sensitive ATPase activity in collecting duct by metabolic alkalosis. *Can J Physiol Pharmacol* 68:1119–1123, 1990
10. Khadouri C, Marsy S, Barlet-Bas C, Cheval L, Doucet A: Effect of metabolic acidosis and alkalosis on NEM-sensitive ATPase in rat nephron segments. *Am J Physiol* 262:F583–F590, 1992
11. Eiam-Ong S, Laski ME, Kurtzman NA, Sabatini S: Effect of respiratory acidosis and respiratory alkalosis on renal transport enzymes. *Am J Physiol* 267:F390–F399, 1994
12. Fejes-Tóth G, Náray-Fejes-Tóth A: Differentiated transport functions in primary cultures of rabbit collecting ducts. *Am J Physiol* 253:F1302–F1307, 1987
13. Náray-Fejes-Tóth G: Immunoselection and culture of rabbit cortical collecting duct cells. *J Tiss Cult Meth* 13:179–184, 1991
14. Fejes-Tóth G, Náray-Fejes-Tóth A: Isolated principal and intercalated cells: Hormone responsiveness and Na^+-K^+-ATPase activity. *Am J Physiol* 256:F742–F750, 1989
15. Fejes-Tóth G, Náray-Fejes-Tóth A: Fluorescence activated cell sorting of principal and intercalated cells of the renal collecting duct. *J Tiss Cult Meth* 13:173–178, 1991
16. Jennings ML, Anderson MP, Monaghan R: Monoclonal antibodies against human erythrocyte band 3 protein. *J Biol Chem* 261:9002–9010, 1986

17. FEJES-TÓTH G, NÁRAY-FEJES-TÓTH A, SATLIN LM, MEHRGUT FM, SCHWARTZ GJ: Inhibition of bicarbonate transport in peanut lectin positive intercalated cells by a monoclonal antibody. *Am J Physiol* 266:F901–F910, 1994
18. HIRSCH S, STRAUSS A, MASOOD K, LEE S, SUKHATME V, GLUCK S: Isolation and sequence of a cDNA clone encoding the 31 kDa subunit of bovine kidney vacuolar H-ATPase. *Proc Natl Acad Sci USA* 85:3004–3008, 1988
19. GISH W, STATES DJ: Identification of protein coding regions by database similarity search. *Nature Genet* 3:266–272, 1993
20. AUSUBEL FM, BRENT R, KINGSTON RE, MOORE DD, SEIDMAN JG, SMITH JA, STRUHL K (editors): *Current Protocols in Molecular Biology*, New York, J. Wiley, 1989, (vol 2) pp. 4.9.1.
21. SCHWARTZ GJ, BARASCH J, AL-AWQATI Q: Plasticity of functional epithelial polarity. *Nature* 318:368–371, 1985
22. BROWN D, HIRSCH S, GLUCK S: Localization of a proton-pumping ATPase in rat kidney. *J Clin Invest* 82:2114–2126, 1988
23. BROWN D, HIRSCH S, GLUCK S: An H^+-ATPase in opposite plasma membrane domains in kidney epithelial cell subpopulations. *Nature* 331:622–624, 1988
24. SCHUSTER VL, FEJES-TÓTH G, NÁRAY-FEJES-TÓTH A, GLUCK S: Colocalization of $H(^+)$-ATPase and band 3 anion exchanger in rabbit collecting duct intercalated cells. *Am J Physiol* 260:F506–F517, 1991
25. GIFFORD JD, ROME L, GALLA JH: H-K-ATPase activity in rat collecting duct segments. *Am J Physiol* 262:F692–F695, 1992